Journal of
MATERIALS RESEARCH



# Synthesis and characterization of $Y_2O_3:Eu^{3+}$ powder phosphor by a hydrolysis technique

Yong Dong Jiang and Zhong Lin Wang
*School of Materials Science & Engineering, Georgia Institute of Technology, Atlanta, Georgia 30332-0245*

Fuli Zhang, Henry G. Paris, and Christopher J. Summers
*Phosphor Technology Center of Excellence, Georgia Tech Research Institute, Atlanta, Georgia 30332-0800*

(Received 9 June 1997; accepted 9 January 1998)

A forced hydrolysis technique is used for preparing $Y_2O_3:Eu^{3+}$ powders at low processing temperatures. The technique uses yttrium oxide, europium oxide, and nitric acid and urea, and has the potential for large-scale production for industrial applications. Several experimental conditions have been examined to optimize the luminescence efficiency. The best result was found to be at 2 mol% Eu doping and a 2 h firing of 1400 °C. Microstructural information provided by x-ray diffraction, scanning electron microscopy (SEM), and transmission electron microscopy (TEM) have been applied to interpret the observed luminescent properties.

## I. INTRODUCTION

High resolution and high efficiency planar displays are one of the national priorities for advanced technology and commercial applications. High efficiency phosphor materials with crystalline monodispersive fine particles are the key for high resolution screens, displays, and flat panels.[1,2] In these applications the quality of the phosphor particles is vitally important, and phosphor pixel size as small as ~10 $\mu$m in diameter are needed for high resolution displays. Such a fine pixel size naturally requires small phosphor particles of less than 5 $\mu$m in diameter. In practice, small size particles may improve aging by forming a densely packed layer. On the other hand, when the particle size becomes smaller than a critical value, the luminescence efficiency decreases. The possible reasons are attributed to increased light absorption and the effect of the surface layer; the latter is believed to quench luminescence.[3] Therefore, developing synthesis techniques that can yield small phosphor particles with a high luminescent efficiency is pertained, and desperately needed.

Yttrium oxide doped with $Eu^{3+}$ ($Y_2O_3:Eu^{3+}$) is one of the main red-emission phosphors used in high efficiency cathode ray tube (CRT) and field emission display (FED).[3] However, preparation of yttria doped with $Eu^{3+}$ by the conventional ceramic method is cumbersome, because it employs a solid state reaction of the oxides at high temperatures with sequential grinding and firing steps. To achieve high quality small particle size of phosphor powders, various preparation routes have been adopted to reduce the reaction temperature, especially wet chemistry methods, such as sol-gel, coprecipitation, etc.[4] Such processes can prepare amorphous particles in aqueous solution at low temperatures (<100 °C) and have the potential to produce powders with improved chemical purity, better chemical homogeneity, and controlled particle size. These properties offer the optimum conditions for subsequent firing procedures and yield well-ordered dispersive phosphor particles with high resolution and high efficiency.

In this paper, a hydrolysis technique using urea[5] has been adopted for synthesis of fine phosphor particles of $Y_2O_3:Eu^{3+}$ at low temperature. This synthesis method can produce spherical particles and control the particle size effectively. The luminescence coefficient of the prepared particles has been measured and the results have been compared with the properties of phosphor particles prepared using different techniques. Various experimental conditions have been tested to optimize the luminescence coefficient of the phosphor powder. Finally, the microstructures of the newly prepared phosphors were examined to determine the dependence of the measured physical properties on the experimental conditions. It has been shown that the crystallinity of the phosphor particles was closely related to the luminescent brightness of the particles.

## II. SYNTHESIS METHOD

In this study, yttrium oxide (99.9%), europium oxide (99.9%), and nitric acid and urea (99%) were used as starting raw materials. $Y(NO_3)_3$ and $Eu(NO_3)_3$ solutions with given concentrations were prepared by dissolving $Y_2O_3$ and $Eu_2O_3$ in nitric acid and diluting with deionized water to 0.05 mol/l. The nitrate solution was mixed with 0.5 M urea solution, then it was filtered and aged for 3 h at 80 °C in an isothermal oven. The

 

precipitates were separated by high speed centrifuging, then washed with de-ionized water to remove residual urea and nitric ions. Finally, the powder was washed with ethanol to remove water. After drying at room temperature, the powder was fired at different temperatures to form crystalline particles. The chemical reactions can be outlined as follows.

During aging, the urea reacted with water to release $OH^-$, the $Y^{3+}$, and $Eu^{3+}$ cations combined with $OH^-$ to form $(Y_{1-x}, Eu_x)(OH)_3$ precipitates, which were amorphous particles at the processing temperature. After firing at different temperatures phosphor particles of $Y_2O_3$ doped with $Eu^{3+}$ were formed. The following reactions were involved in the processing of the particles[6]:

$$CO(NH_2)_2 + 3H_2O \rightarrow CO_2 \uparrow + 2NH_4^+ + 2OH^-,$$

$$(1 - x)Y^{3+} + xEu^{3+} + 3OH^- \rightarrow (Y_{1-x}, Eu_x)(OH)_3 \downarrow,$$

$$2(Y_{1-x}, Eu_x)(OH)_3 \rightarrow (Y_{1-x}, Eu_x)_2O_3 + 3H_2O.$$

The crystal phase was determined by x-ray powder diffraction using a Philips PW 1800 diffractometer, and the morphology of the particles before and after firing was observed by scanning electron microscopy (SEM) using a Hitachi S-800 SEM. The grain structure was examined by transmission electron microscopy at 200 kV using a Hitachi HF 2000 TEM equipped with a field emission source.

## III. CHARACTERIZATION OF LUMINESCENT PROPERTIES

As the most important property of the phosphor particles, the luminescence efficiency must be measured as a function of firing temperature, $Eu_2O_3$ doping concentration, and electron voltage, respectively. These measurements were carried out by impinging a powder sample with a continuous electron beam and measuring the brightness at 45° on deep powder patches. The detailed measurement technique has been given elsewhere.[7] Brightness data were converted into intrinsic efficiency with respect to electron beam energy according to

$$\text{efficiency (lm/W)} = \frac{100\pi L_0}{jV},$$

where $L_0$ is the brightness in $Cd/m^2$, $j$ is the electron beam current density in $\mu A/cm^2$, and $V$ is the accelerating voltage in volts.

Figure 1 shows the relationship between the luminescent efficiency of the phosphor particles (fired at 1000 °C for 2 h) and the molar concentration of the $Eu_2O_3$ dopant as a function of accelerating voltage. The efficiency has a maximum at a doping concentration of 2 mol % $Eu_2O_3$, but excess $Eu_2O_3$ doping decreases the efficiency. Therefore, the 2 mol % $Eu_2O_3$ is the optimum concentration for improving the luminescent efficiency in our experiments. This parameter was thus fixed for all of the following experiments. Figure 2 shows the luminescent efficiency of particles fired at 1000 °C via firing time. The particles fired at 1000 °C for 2 h had the highest efficiency, while an increase in firing time resulted in a decrease in the efficiency. This behavior has also been observed for phosphor powders prepared by other techniques, but the reason for this behavior is unclear.

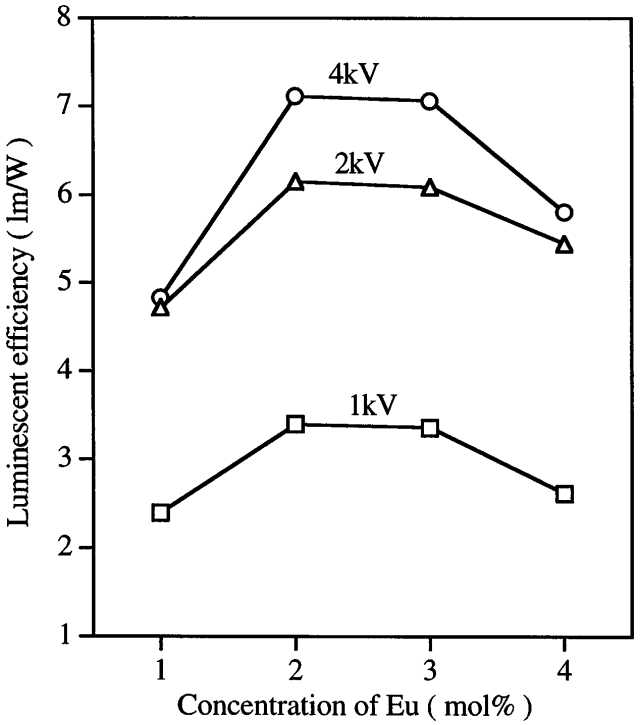


FIG. 1. Luminescent efficiency of the newly synthesized $Y_2O_3:Eu^{3+}$ powders as a function of the molar doping concentration of $Eu_2O_3$. The sample was fired at 1000 °C for 2 h.

Figure 3 shows the luminescent efficiency of the particles with 2 mol % $Eu_2O_3$ dopant fired for 2 h as a function of firing temperature. It is apparent that the efficiency increases with increasing firing temperature, and shows an increase of ~70% when the firing temperature increases from 1000 to 1400 °C, where it reaches the maximum (about 11.6 lm/W). However, a further increase in firing temperature above 1400 °C results in a decrease in the efficiency. For comparison purposes, luminescence efficiency measured from a standard specimen of $Y_2O_2S:Eu$, which has been used as the standard in many of our studies, is also plotted in the figure. It is apparent that the $Y_2O_3:Eu^{3+}$ powders prepared by the hydrolysis technique presented here have higher efficiency for all electron accelerating voltages. At 4 kV accelerating voltage the efficiency of the $Y_2O_3:Eu^{3+}$ powder (11.6 lm/W) is about 50% higher than that of the $Y_2O_2S:Eu$ powder (7.9 lm/W). This is an endorsement to the performance of the newly prepared samples.

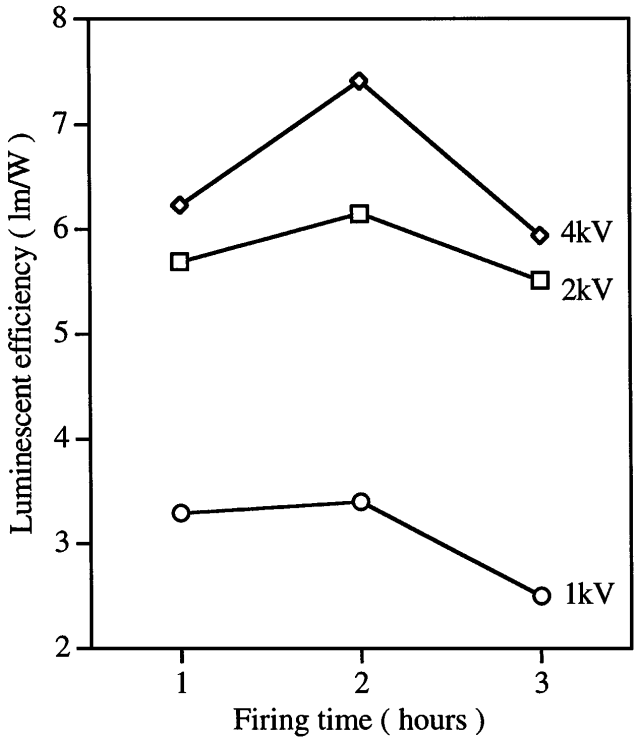


FIG. 2. Luminescent efficiency of the $Y_2O_3:Eu^{3+}$ powders fired at 1000 °C for different lengths of time. $Eu_2O_3$ concentration was 2 mol %.

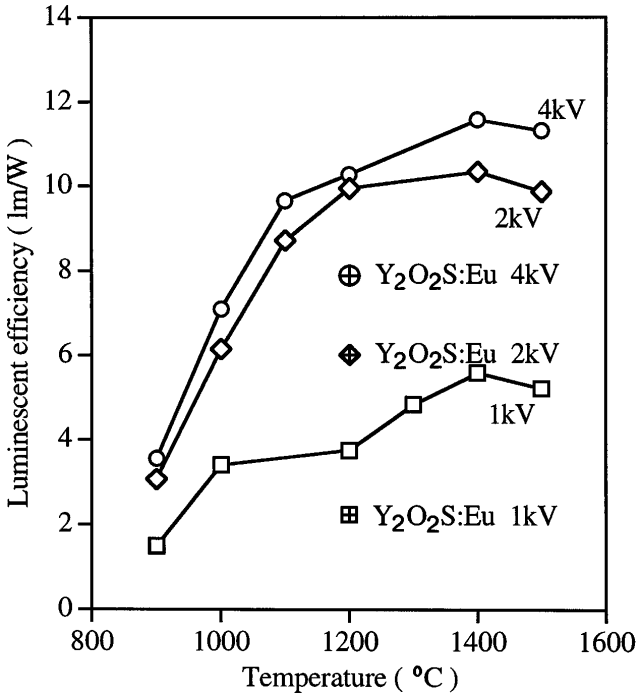


FIG. 3. Luminescent efficiency of the $Y_2O_3:Eu^{3+}$ powders as a function of the firing temperature and the electron voltages. $Eu_2O_3$ concentration was 2 mol % and the firing time was 2 h. The efficiency measured from a standard specimen of $Y_2O_2S:Eu$ is also shown for comparison.

As a summary, the highest luminescent efficiency is achieved for 2 mol % Eu doping, 2 h firing at 1400 °C. The microstructural characterization described in the next session explains the structural evolution that induces this behavior. Figures 1–3 show a common feature: the luminescent efficiency increases with increasing the electron accelerating voltage. The low efficiency at low voltages is ascribed to a nonluminescent surface layer (dead layer) and charge buildup.[4]

## IV. MICROSTRUCTURE CHARACTERIZATION

The as-prepared precursor hydroxide particles are amorphous, and their crystallinity is expected to increase with increasing firing temperature. To determine the crystallization behavior of the specimens fired at different temperatures, x-ray diffraction was employed. Figure 4(a) shows the x-ray spectra of the particles fired at different temperatures. With increasing the firing temperature, the (222) peak shifts slightly toward lower angle [Fig. 4(b)], indicating an increase in lattice parameters. It is anticipated that with increasing firing temperature more $Eu_2O_3$ would be incorporated or incorporated more completely into the $Y_2O_3$ lattice. Since the lattice parameter of $Eu_2O_3$ is slightly (2.4%) larger than that of $Y_2O_3$, the diffraction peak is expected to shift to a lower angle. Furthermore, the intensities of the main peaks increase in reference to the background with increasing of firing temperature, and the full-width at half-maximum (FWHM) of the (222) peaks of the particles fired at high temperatures are smaller than those of the particles fired at low temperatures. This means that the particles fired at higher temperatures exhibit a higher crystallinity than those fired at lower temperatures, resulting in the increased luminescent efficiency.

The morphology of the particles before and after firing was examined by SEM (Fig. 5) and TEM (Fig. 6). It can be seen from the SEM image that most of the particles are spherical, but after firing more agglomerations are observed, particularly for the ones fired at higher temperatures. The size distributions of the particles fired at different temperatures were calculated based on the SEM and TEM images for a total of 500 particles in each case. The particle size exhibits a sharp increase with increasing the firing temperature (Fig. 7), especially at higher temperatures.

The evolution in the intrinsic microstructure of the powders is examined using TEM. Figure 6 shows the TEM images and the corresponding electron diffraction patterns of the particles fired at two different temperatures. The diffraction pattern recorded from the powder fired at 900 °C is composed of continuous rings, while the one fired at 1200 °C shows some discrete spots. This means that the average particle size increases with

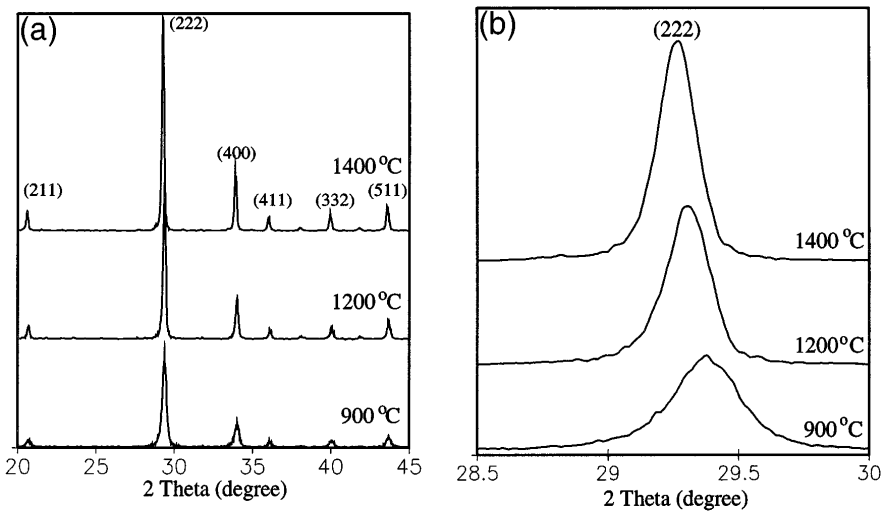


FIG. 4. (a) X-ray diffraction spectra of $Y_2O_3:Eu^{3+}$ particles fired at different temperatures, showing the increased crystallinity of the particles as the temperature increases. (b) An enlargement of the (222) peak, showing the reduced FWHM and the peak shift as the temperature increases.

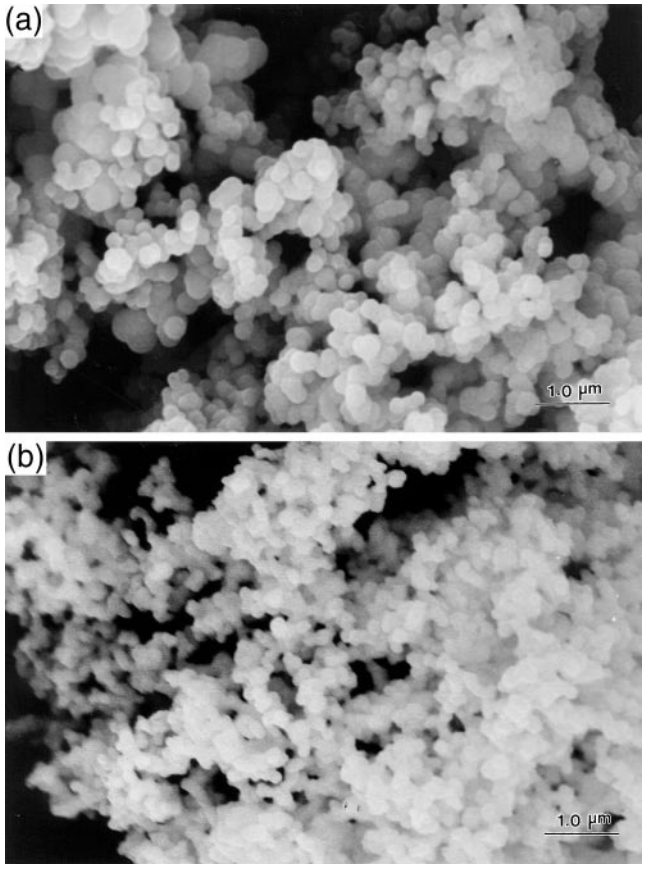


FIG. 5. Morphology of the $Y_2O_3:Eu^{3+}$ particles (a) before and (b) after firing at 1200 °C for 2 h.

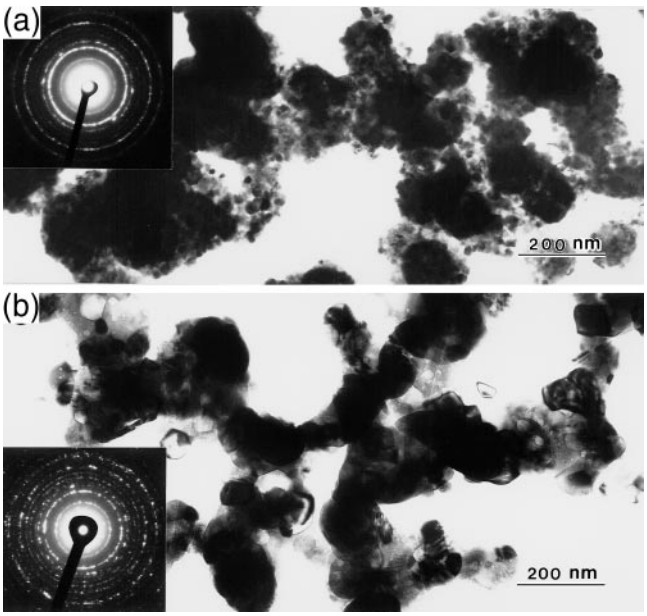


FIG. 6. TEM images and the corresponding electron diffraction patterns for the powders fired at (a) 900 °C and (b) 1200 °C, respectively.

increasing the firing temperature. The smaller particles have a relatively larger surface-to-volume ratio, resulting in more light scattering at the surfaces and interfaces; thus, the luminescent efficiency is lower, in agreement with the measurement shown in Fig. 3.

The improved crystallinity and quality of the particles as the firing temperature increases is clearly shown by the high-resolution TEM images, as given in Fig. 8. There are many nanocrystals contained in each particle in the specimen fired at 900 °C [Fig. 8(a)]. This is a process of structural evolution from amorphous to an ordered crystalline state. The size of the nanoparticles increases as the firing temperature increases [Fig. 8(b)], and at 1400 °C, each particle is a single crystalline phase [Fig. 8(c)]. Therefore, it is natural that the luminescent efficiency is higher.

Furthermore, at lower firing temperatures, luminescent efficiencies drop due to the nonperfect bulk

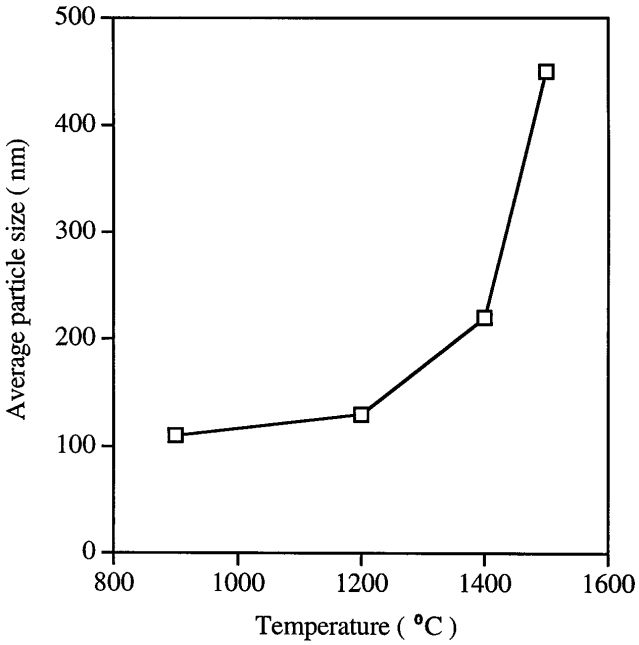


FIG. 7. Average particle size calculated from TEM images for the specimens fired at different temperatures.

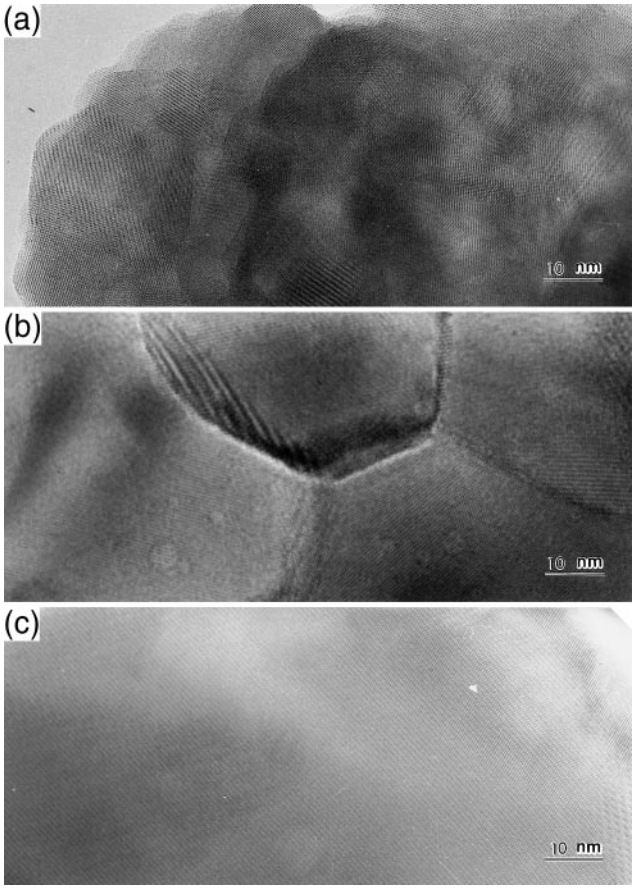


FIG. 8. High-resolution TEM images recorded from the powders fired at (a) 900 °C, (b) 1200 °C, and (c) 1400 °C, respectively.

formation, e.g., the formation of the killer centers or the imperfect cooperation of the activator ions.[8] When the firing temperature increases, the particle size increases, the surface area per unit volume decreases, and light scattering decreases as well; thus the efficiency is improved. However, at higher firing temperatures more hard agglomerations were observed, especially at 1500 °C (Fig. 9). The hard agglomerations lead to lower particle packaging densities and a high concentration of packing voids; thus, a large amount of light is scattered by the surfaces of the voids.[9] This might be the reason why the particle fired at 1500 °C has a lower luminescent efficiency than the one fired at 1400 °C.

## V. CONCLUSIONS

In this paper, a new hydrolysis technique is reported for preparing $Y_2O_3:Eu^{3+}$ powders at low processing temperatures. The technique has the potential to be expanded to large-scale production. Several experimental conditions have been examined to optimize the luminescence efficiency, and the best result was found to be at a doping of 2 mol% $Eu_2O_3$ and a 2 h firing at 1400 °C. With increasing firing temperature, the particle size and luminescent efficiency increased to a maximum at a firing temperature of 1400 °C. The efficiency of the newly prepared powders was 20–40% higher than the standard specimen.

Microstructure analysis using x-ray diffraction, SEM, and TEM has shown that at low firing temperatures, the particles are composed of many nanoclusters; increasing firing temperature results in an increase in

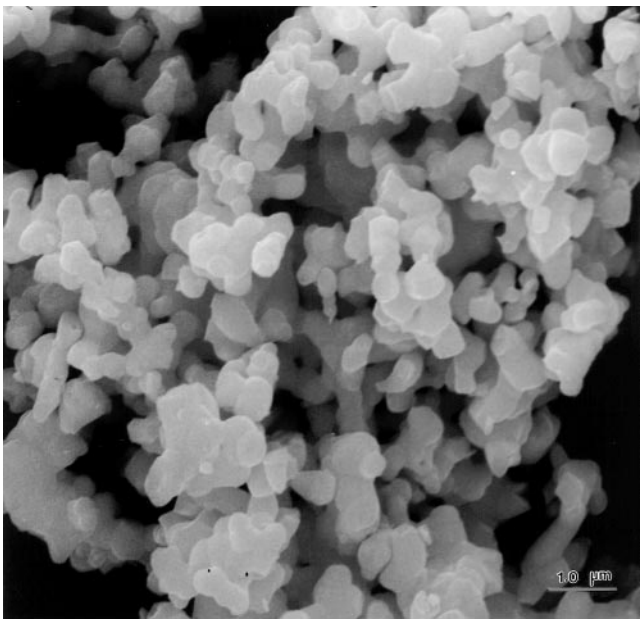


FIG. 9. SEM image recorded from the $Y_2O_3:Eu^{3+}$ particles fired at 1500 °C for 2 h, showing the formation of hard agglomerations.

the size of the nanoclusters, until finally each particle becomes a single crystalline grain at 1400 °C. The increase in crystallinity and single crystal grain size significantly reduces the light scattering at surfaces and interfaces, resulting in higher luminescence efficiency. On the other hand, at higher firing temperatures hard agglomerations are formed with lower packing density and a higher density of voids, leading to the observed lower luminescent efficiency at 1500 °C.

## ACKNOWLEDGMENTS

We are grateful to Dr. Z. C. Kang for his many stimulating discussions. This research was supported by the Phosphor Technology Center of Excellence at Georgia Institute of Technology and ARPA Contract No. MDA 972-93-1-0030.

## REFERENCES

1. R. P. Rao, J. Electrochem. Soc. **143**, 189 (1996).
2. S. Erdie, R. Roy, *et al.*, Mater. Res. Bull. **30**, 145 (1995).
3. H. Yamamoto, J. SID **4**, 165 (1996).
4. M. Kottaisamy, K. Jeyakumar, *et al.*, Mater. Res. Bull. **31**, 1013 (1996).
5. E. Matijevic and W. P. Hsu, J. Colloid Interface Sci. **118**, 506 (1987).
6. Y. Huang and C. Guo, Powder Technol. **72**, 101 (1992).
7. J. A. Cooper, Thesis of Master Degree of Science, School of Materials Science and Engineering, Georgia Institute of Technology (1996).
8. T. Welker, Electrochem. Soc. Meeting Extended Abstract **91-2**, 973 (1991).
9. Kyoichioki and Lyuji Ozawa, J. SID **3**, 51 (1995).